Conical Second Harmonic Generation in a Two-Dimensional $\chi^{(2)}$ Photonic Crystal: A Hexagonally Poled $LiTaO_3$ Crystal

P. Xu, S. H. Ji, S. N. Zhu,* X. Q. Yu, J. Sun, H. T. Wang, J. L. He, Y. Y. Zhu, and N. B. Ming
National Laboratory of Solid State Microstructures, Nanjing University, Nanjing, 210093, China
(Received 9 February 2004; published 23 September 2004)

A new type of conical second-harmonic generation was discovered in a 2D $\chi^{(2)}$ photonic crystal—a hexagonally poled $LiTaO_3$ crystal. It reveals the presence of another type of nonlinear interaction—a scattering involved optical parametric generation in a nonlinear medium. Such a nonlinear interaction can be significantly enlarged in a modulated $\chi^{(2)}$ structure by a quasi-phase-matching process. The conical beam records the spatial distribution of the scattering signal and discloses the structure information and symmetry of the 2D $\chi^{(2)}$ photonic crystal.

DOI: 10.1103/PhysRevLett.93.133904 PACS numbers: 42.65.Ky, 42.25.Fx, 42.70.Mp

Recently several novel classes of noncollinear parametric interactions were discovered, such as the ring-shaped second-harmonic generation (SHG) excited by a Bessel beam in a periodically poled KTP crystal [1], the hollow beam generated by the frequency difference in a periodically poled $LiTaO_3$ crystal [2], the ring-shaped SH generated from a SBN crystal having an antiparallel domain when a fundamental wave is propagated in its crystallographic c axis [3], and so on. On the other hand, ring-shaped harmonic patterns were even produced from either a single domain crystal [4] or an isotropic material [5]. In all the cases above, conical patterns indicated that either the single fundamental beam was particularly prepared or an additional beam was required in addition to the incident fundamental beam.

The nonlinear crystal with a modulated nonlinear susceptibility tensor $\chi^{(2)}$ was called a quasi-phase-matching (QPM) material. The concept was first referred to by Armstrong [6] and Franken and Ward [7] independently. In 1998, Berger extended the QPM study from one dimension (1D) to 2D [8], and proposed the concept of an $\chi^{(2)}$ photonic crystal in order to contrast and compare it with a regular photonic crystal having a periodic linear susceptibility. Since then, the concept of a $\chi^{(2)}$ photonic crystal has been gradually accepted in the nonlinear optics community. A number of theoretical and experimental results show that the $\chi^{(2)}$ photonic crystal, in particular, the 2D one, provides a valuable platform to study light-matter interaction in a highly nonlinear regime [9–12].

In this Letter, we report a novel nonlinear optical phenomenon—a conical second-harmonic (SH) beam, generated from a 2D $\chi^{(2)}$ photonic crystal—a hexagonally poled $LiTaO_3$ (HPLT) crystal. The conical SH beam emerged when the HPLT was illuminated with a z-polarized fundamental beam with no special requirements. The conical beams were visualized as rings when projected onto a screen behind the crystal, and were presented in axial symmetry or mirror symmetry when the fundamental beam propagated along a symmetrical axis of the hexagonal structure. This reveals the presence of another type of nonlinear interaction—a scattering involved optical parametric generation. The interaction is greatly enhanced by a QPM process in the 2D $\chi^{(2)}$ photonic crystal; thus, the infrared scattering signal (ω) is converted to a visible band (2ω) through mixing with the incident wave (ω). Further study confirms that the conical beam records the spatial distribution of the scattering signal and reveals the structure information of the 2D $\chi^{(2)}$ photonic crystal.

In the experiments the 2D $\chi^{(2)}$ photonic crystal is a hexagonally poled $LiTaO_3$ crystal fabricated by a field poling technique [13]. Figure 1(a) shows its domain structure slightly etched in acids. The nearly circularly inverted domains (with $-\chi^{(2)}$) distribute regularly in a $+\chi^{(2)}$ background with $a = 9.05$ μm and a reversal factor of ~40%. No domain merging was found across the sample dimensions of 1.55 cm (x) × 1.55 cm (y). Figure 1(b) is the corresponding reciprocal space, in which each reciprocal vector has six equivalent ones [9].

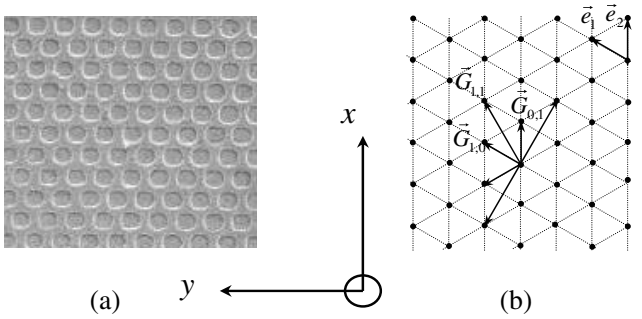

FIG. 1. (a) HPLT crystal and its domain structure. (b) Reciprocal lattice and reciprocal vectors of the HPLT crystal. In our experiments the fundamental beam propagated in the $+x$ and the $+y$ directions, respectively. Here are two sets of the mentioned reciprocal vectors clarified by the magnitude, $4\pi/\sqrt{3}a$ and $4\pi/a$, respectively.

The phase-matching condition for SHG in a 2D $\chi^{(2)}$ photonic crystal is generally written into

$$\vec{k}_2 - 2\vec{k}_1 - \vec{G}_{m,n} = 0, \quad (1)$$

where $\vec{G}_{m,n} = \frac{4\pi}{\sqrt{3}a}(\sqrt{m^2 + n^2 + m \cdot n})$ is the reciprocal vector of the 2D hexagonal lattice with the lattice parameter of a, and the subscripts m and n are integers, representing the order of the reciprocals. In Eq. (1), $\vec{k}_1$ represents the incident beam providing two fundamental waves, and three vectors, $\vec{k}_1$, $\vec{k}_2$, and $\vec{G}_{m,n}$, may be collinear or noncollinear to one another.

We performed a detailed experimental study of SHG for this HPLT in a single-pass scheme. The fundamental wave source is a tunable optical parametric oscillator (PL9010, Continuum, Santa Clara, CA). Its output, having a nearly Gaussian profile, can be tuned from ultraviolet (200 nm) to infrared (1700 nm) with the pulse width of ~5 ns, the linewidth ≤ 0.075 cm^{-1}, and the repetition rate of 10 Hz. The z-polarized fundamental beam was weakly focused with a beam waist of 0.1 mm inside the crystal. The confocal parameter $Z_0 \approx 6$ cm for the system. It is much longer than the length of the sample of 1.55 cm; therefore, the divergence of $\vec{k}_1$ inside the crystal is negligible.

At the beginning, the fundamental $\vec{k}_1$ propagated along the x direction of the HPLT crystal. By changing the wavelength of $\vec{k}_1$, two kinds of axial SH beams $\vec{k}_2$ were found as expected according to Eq. (1). The first one was a single axial beam collinear with $\vec{k}_1$, and the involved reciprocal $\vec{G}_{m,n}$ was parallel to $\vec{k}_1$. The other one was a pair of axial beams symmetrical from $\vec{k}_1$ in the x-y plane [9]. In this case, a pair of symmetrical reciprocals from $\vec{k}_1$ participated in the noncollinear QPM process. In the visible band, the number of such an axis beam at different wavelengths adds up to be about 20. It is caused by the participation of different reciprocals. All results are in good agreement with the theoretical estimations by Eq. (1). For simplicity, two of them are studied in detail. One occurred at SH $\lambda_2 = 532$ nm in a single axial beam by $\vec{G}_{0,1}$ and the other at $\lambda_2 = 466.5$ nm in a pair of axial beams by $\vec{G}_{1,1}$ and its mirror image.

In a subsequent experiment, new effects were exhibited as $\vec{k}_1$ was detuned from the above matching points toward a longer wavelength. We found that the axial SH beams disappeared, yet, instead, a new type of beam, a conical SH beam, emerged from this HPLT. These beams exhibited circular rings when projected onto a screen as shown in Fig. 2. The inset of Fig. 2(a) is a single circular ring at $\lambda_2 = 533$ nm. It developed from the single axial SH beam at 532 nm. Its center overlapped with the projection point of $\vec{k}_1$. Its radius increased with the increase of the fundamental wavelength λ_1.

Another kind of conical SH beams, $\vec{k}_2$, emerged from the crystal in pairs as shown in the inset of Fig. 2(b). Two rings have the identically symmetrical angles from $\vec{k}_1$. Similarly, these two rings decreased their radiuses synchronously with the decreasing of λ_1. During this process, a bright spot appeared on the inner side of each ring at a specified $\lambda_1 = 933$ nm. They were the SH of λ_1, fulfilling Eq. (1) in noncollinear scheme. As the rings reduced in radius with the further decrease of λ_1, these two bright spots on the rings disappeared due to their phase-matched condition to be destroyed. The rings shrunk to their centers as $\lambda_1 = 930$ nm, forming another two weaker bright spots at $\lambda_2 = 465$ nm. Both the ring and the spot disappeared as λ_1 was tuned down to shorter than 930 nm. α_1 and α_2 are defined in Fig. 3(b) as the angles of $\vec{k}_2$ to $\vec{k}_1$ on the x-y plane and the dependence on λ_2 is shown in Fig. 2(b). The conical SH beams and latter two weak bright spots mentioned above cannot be explained using Eq. (1). Obviously, they occur through a different mechanism.

A comprehensive interpretation for the conical SH beams can be given by introducing an additional funda-

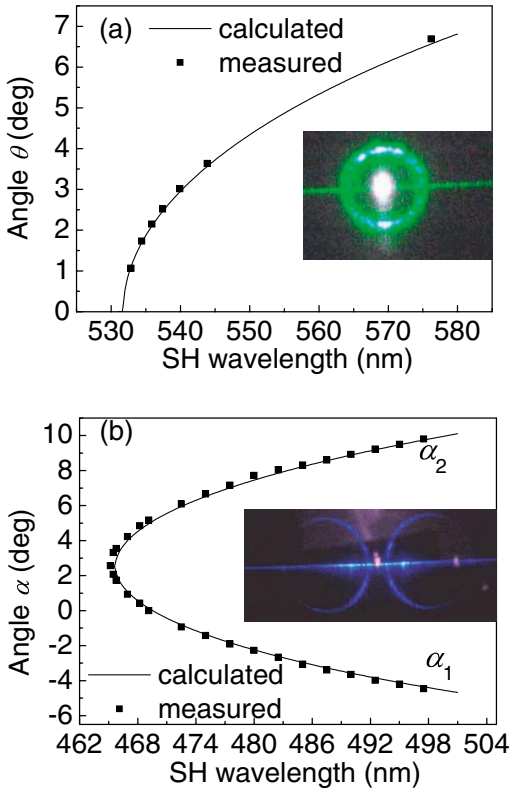

FIG. 2 (color online). (a) The angle θ as a function of λ_2 for a single ring. (b) The angle α as a function of λ_2 for a pair of rings (see text). The insets of (a) and (b) are the axially symmetrical ring and the mirror-symmetrical ring, respectively. The bright spot at the ring center in (a) is the projection of $\vec{k}_1$.

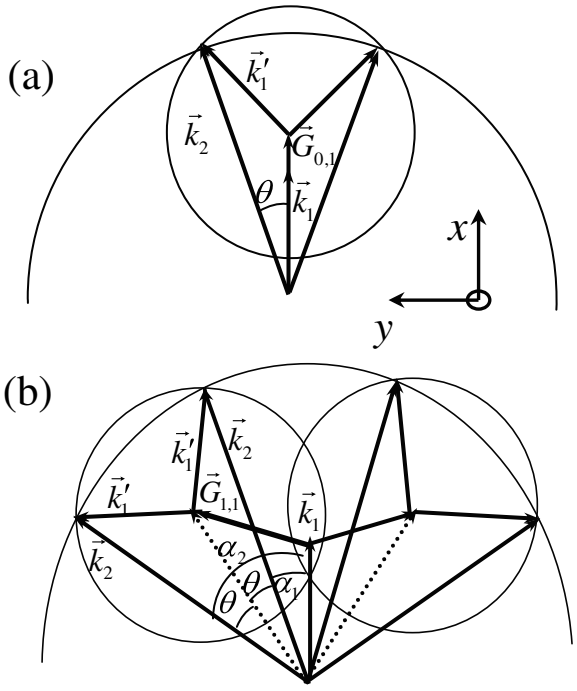

FIG. 3. Phase-matching geometries for (a) the axially symmetrical ring and (b) the mirror-symmetrical rings.

mental wave $\vec{k}_1'$. Taking $\vec{k}_1'$ to be noncollinear to $\vec{k}_1'$, Eq. (1) can be more generally written as

$$\vec{k}_2 - \vec{k}_1 - \vec{k}_1' - \vec{G}_{m,n} = 0. \tag{2}$$

The equation degenerates into Eq. (1) when $\vec{k}_1' = \vec{k}_1$. In order to obtain a conical SH beam, $\vec{k}_1'$ has to present a continuously and symmetrically spatial distribution from $\vec{k}_1$. In our experiment $\vec{k}_1$ was loosely focused and no second fundamental beam was directed onto the crystal; therefore, $\vec{k}_1'$ can be provided from $\vec{k}_1$ by scattering. $\vec{k}_1'$ has a small scattering angle from $\vec{k}_1$. The scattering may arise mainly from domain walls and other imperfections on the surface and inside the crystal and does not change the wavelength of light [14]. The scattering effect has been observed by nonlinear interactions in some homogeneous crystals [15]. Now, however, it is clarified in a 2D $\chi^{(2)}$ photonic crystal in a QPM scheme, which leads to a new class of SH pattern—a reciprocal-dependent conical SH beam.

Geometries for the generation of two kinds of conical beams at normal incidence onto the HPLT are shown in Figs. 3(a) and 3(b), respectively. In Fig. 3(a), $\vec{k}_1 \parallel \vec{G}_{0,1}$, and $\vec{k}_1'$ exhibits a forward axis-symmetrical distribution around $\vec{k}_1$. The generated SH $\vec{k}_2$ obeying Eq. (2) forms a conical beam. The angle θ between $\vec{k}_1$ and $\vec{k}_2$ is given by

$$\cos(\theta) = \frac{|\vec{k}_2|^2 + |\vec{k}_1 + \vec{G}_{m,n}|^2 - |\vec{k}_1|^2}{2|\vec{k}_2| \cdot |\vec{k}_1 + \vec{G}_{m,n}|}, \tag{3}$$

where $\vec{G}_{m,n}$ is $\vec{G}_{0,1}$ for the present case. Because $\cos\theta \leq 1$, the equation implies that the conical beam just occurs as λ_1 is longer than a critical wavelength at which $\theta = 0$. The angle θ increases with λ_1. The curve calculated based on Eq. (3) fits the measured values well as shown in Fig. 2(a). Figure 3(b) shows another phase-matching geometry that leads to the generation of the pair of rings on the screen shown as the inset of Fig. 2(b), where $\vec{G}_{m,n}$ is $\vec{G}_{1,1}$ or its mirror image. These two rings are symmetrical from $\vec{k}_1$, as well as from the x axis. Equation (3) is still valid for this phase-matching geometry. However, here θ is the angle between $\vec{k}_2$ and $\vec{k}_1 + \vec{G}_{1,1}$ instead of $\vec{k}_1$ [see Fig. 3(b)]. Obviously, the projection spot of $\vec{k}_1 + \vec{G}_{1,1}$ on the screen is the center of rings, and it is invisible generally. The center changes its position with λ_1 because $\vec{k}_1 + \vec{G}_{1,1}$ is a function of λ_1. The pair of rings reduce in radius with the shortening of λ_1, and, lastly, the conical beams $\vec{k}_2$ shrink into two axial beams with $\theta = 0$ when the $\vec{k}_2$, $\vec{k}_1'$, and $\vec{k}_1 + \vec{G}_{1,1}$ three vectors are collinear. At that moment two symmetrical bright spots appear on the screen.

It should be mentioned that $LiTaO_3$ is a birefringence crystal. The ring on the screen should be elliptical and not circular. However, the birefringence of the crystal is so small that the calculated result shows the deviation from a circle amounts to about 10^{-4} °, and, therefore, is negligible in the experiment.

In addition to the two cases of rings studied above, there are many other rings observed in the visible band. They differ little but correspond to different reciprocals. As the HPLT was rotated by 90° around the z axis and $\vec{k}_1$ propagated in the y direction, two pairs of conical SH

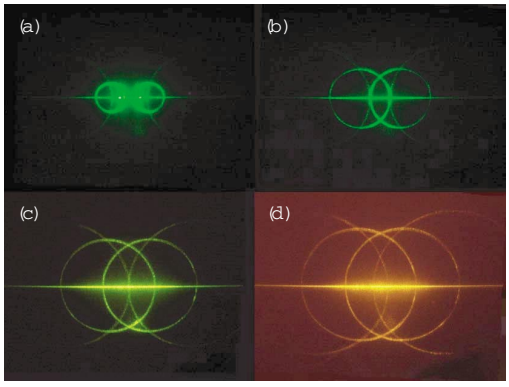

FIG. 4 (color online). The projection of the mirror-symmetrically conical SH beams on the screen ($\vec{k}_1 \parallel y$ axis): (a) $\lambda_1 = 1.12$ μm; (b) $\lambda_1 = 1.13$ μm; (c) $\lambda_1 = 1.15$ μm; (d) $\lambda_1 = 1.17$ μm.

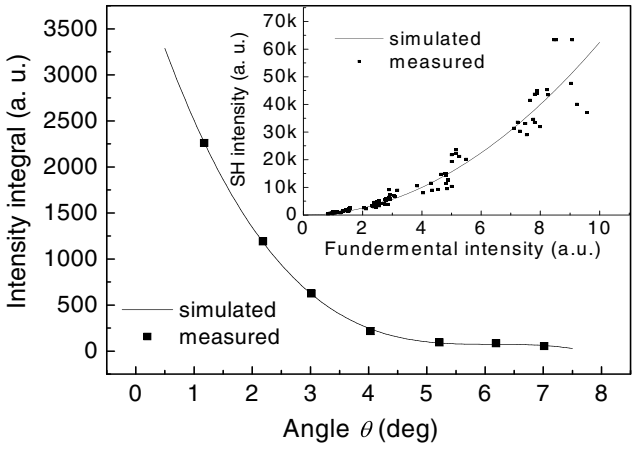

FIG. 5. The intensity integral of the axially symmetrical ring as a function of θ. The inset shows the dependence of $I(2\omega)$ on $I(\omega)$ at $\theta = 0.5°$.

beams with different azimuths occurred simultaneously. They are, respectively, associated with two sets of reciprocals, $\vec{G}_{1,0}$ and its mirror image, and $\vec{G}_{1,1}$ and its mirror image, the former for two inner rings and the latter for two outer rings. Two pairs of rings and their evolution with λ_1 is shown in Figs. 4(a)–4(d).

We measured the intensity dependence of an axially symmetric ring [Fig. 2(a)] on θ. The intensity integral along the ring decreased considerably with the increasing of θ as shown in Fig. 5, which implies the SHG efficiency is strongly dependent on the distribution of scattering light. Strong scattering occurs when $\theta < 4°$ in the sample. For the pair of rings, the intensity of the each part of the ring is different, depending on the azimuth relative to $\vec{k}_1$ [see Fig. 3(b)]. Solving the nonlinear wave equation, the SH intensity can be expressed as $I(L, 2\omega) \propto I(\omega)I'(\omega)L^2$, where L is the interaction volume and $I(\omega)$ the intensity of $\vec{k}_1$. Scattering intensity $I'(\omega) = \gamma I(\omega)$, where γ is the scattering coefficient. Thus harmonic intensity $I(2\omega)$ is directly proportional to $I(\omega)^2$. The inset of Fig. 5 shows the measured total intensity of ring $I(2\omega)$ dependence on $I(\omega)$ at $\theta = 0.5°$. The fit curve in the figure confirms the square law dependence of $I(2\omega)$ on $I_1(\omega)$. We obtained a maximum average power of $\sim$3.55 mW at the input power of 25.7 mW with an efficiency of $\sim$14%.

Recent parametric scattering patterns, such as the ring and the line, were found in photorefractive crystals, such as Y, Fe codoped $LiNbO_3$ [16], Cr doped SBN [17], etc. $LiTaO_3$ is one of the photorefractive crystals. We performed an elevated temperature measurement up to 170 °C. No obvious change was found in the ring intensity except that the ring reduced in radius with temperature. It was reported that the photorefractive effect in $LiTaO_3$ could be greatly depressed over 80 °C, so the conical SH beam could not originate from this effect.

The conical SH beam generated in a 2D $\chi^{(2)}$ photonic crystal contains useful information about the quality and microstructure of crystal and, therefore, can be viewed as a sensitive, contact-free probe for the characterization of a nonlinear photonic crystal and for the study of light scattering in a crystal. For example, one may obtain the angular distribution of scattering light inside the crystal from the results as shown in Fig. 5. We also found the conical beams generated from 1D $\chi^{(2)}$ crystals like PPLN and PPLT. For a 1D quasiperiodical structure, the pattern on the screen is a set of concentric rings. They exhibit a quasiperiodical ratio at radius. Therefore, the patterns can disclose the structure information of the $\chi^{(2)}$ crystal.

It is worth noting that the scheme in this Letter provides new possibilities for engineering nonlinear interactions. It also demonstrates a new approach for generating a conical beam by frequency conversion. However, the brightness of the conical beam can be significantly enhanced by intentionally inducing the imperfections on the surface and inside the crystal or by using another laser with proper divergence, for some particular purposes.

This work was supported by grants for the National Advanced Materials Committee of China and for the State Key Program for Basic Research of China, as well as by the National Natural Science Foundation of China under Grant No. 90201008 and Natural Science Foundation of Jiangsu under Grant No. BK2002202.

*Email address: zhusn@nju.edu.cn

[1] A. Piskarskas *et al.*, Opt. Lett. **24**, 1053 (1999).
[2] G. Giusfredi *et al.*, Phys. Rev. Lett. **87**, 113901 (2001).
[3] A. R. Tunyagi *et al.*, Phys. Rev. Lett. **90**, 243901 (2003).
[4] J. A. Giordmaine, Phys. Rev. Lett. **8**, 19 (1962).
[5] K. D. Moll *et al.*, Phys. Rev. Lett. **88**, 153901 (2002).
[6] J. Armstrong *et al.*, Phys. Rev. **127**, 1918 (1962).
[7] P. A. Franken and J. F. Ward, Rev. Mod. Phys. **35**, 23 (1963).
[8] V. Berger, Phys. Rev. Lett. **81**, 4136 (1998).
[9] N. G. R. Broderick *et al.*, Phys. Rev. Lett. **84**, 4345 (2000).
[10] N. G. R. Broderick *et al.*, J. Opt. Soc. Am. B **19**, 2263 (2002).
[11] L. H. Peng *et al.*, Appl. Phys. Lett. **83**, 3447 (2003).
[12] S. N. Zhu, Y. Y. Zhu, and N. B. Ming, Science **278**, 843 (1997).
[13] S. N. Zhu *et al.*, J. Appl. Phys. **77**, 5481 (1995).
[14] B. Bittner *et al.*, J. Phys. Condens. Matter **14**, 9013 (2002).
[15] K. U. Kasemir and K. Betzler, Appl. Phys. B **68**, 763 (1999).
[16] M. Goulkov *et al.*, Phys. Rev. Lett. **86**, 4021 (2001).
[17] M. Goulkov *et al.*, Phys. Rev. Lett. **91**, 243903 (2003).